DOI: 10.17344/acsi.2020.6248 *Acta Chim. Slov.* **2021,** *68,* 548–561

Scientific paper

Efficient Removal of Aqueous Manganese (II) Cations by Activated Opuntia Ficus Indica Powder: Adsorption Performance and Mechanism

Boutheina Djobbi,[1] Ghofrane Lassoued Ben Miled,[1] Hatem Raddadi[2] and Rached Ben Hassen[1,*]

[1] *Laboratory of Materials and Environment for Sustainable Development, LR18ES10, University of Tunis El Manar, ISSBAT, 9, Avenue Dr. Zoheir Safi, 1006 Tunis, Tunisia.*

[2] *National Sanitation Office of Tunis, Purification Department, Sidi Salah street, Chotrana, Ariana. Tunisia.*

* *Corresponding author: E-mail: rached.benhassen@issbat.utm.tn*

Received: 07-08-2020

Abstract

The adsorption of manganese ions from aqueous solutions by pure and acid-treated *Opuntia ficus indica* as natural low-cost and eco-friendly adsorbents was investigated. The adsorbents' structures were characterized by powder X-ray diffraction and infrared spectroscopy. Specific surface areas were determined using the Brunauer-Emmett-Tell equation. The study was carried out under various parameters influencing the manganese removal efficiency such as pH, temperature, contact time, adsorbent dose and initial concentration of manganese ion. The maximum adsorption capacity reached 42.02 mg/g for acid-treated *Opuntia ficus indica*, and only 20.8 mg /g for pure *Opuntia ficus indica*. The Langmuir, Freundlich and Temkin isotherms equations were tested, and the best fit was obtained by the Langmuir model for both adsorbents. The thermodynamic study shows that chemisorption is the main adsorption mechanism for the activated adsorbent while physisorption is the main adsorption mechanism for the pure adsorbent. The kinetics of the adsorption have been studied using four kinetics models of pseudo-first order, pseudo-second order, Elovich and intra-particle diffusion. Structural analyses indicate the appearance of MnO_x oxides on the cellulose fibers. The adsorption mechanisms consist of an electrostatic interaction followed by oxidation of the Mn (II) to higher degrees, then probably by binding to the surface of the adsorbent by different C-O-MnO_x bonds.

Keywords: Adsorption mechanism; manganese; removal efficiency; *Opuntia ficus indica*; environmental.

1. Introduction

Unlike organic pollutants, which are mostly affected by biological degradation, the hazards of heavy metals are related to their inability to degrade into non-harmful end products. It can cause acute and chronic damage to various organisms if present. Therefore, the removal of heavy metals from water and wastewater is crucial to protect the health of living organisms. Heavy metals are naturally present in the ecosystem, and their recent increase is attributed to the effluents of many industries, such as metal plating facilities, mining operations and tanneries. Manganese (Mn) is the third most abundant transition metal in nature, usually present in surface water and groundwater as a divalent ion (Mn^{2+}). It is considered as pollutant mainly because of its organoleptic properties.[1–6] Its removal from an aqueous solution is a serious problem in many countries as it is one of the most difficult elements to remove.[7] Contact of manganese-contaminated water with air enhances the oxidation of Mn (II) to Mn (IV). The Mn (IV) precipitate can stain utensils and clothing,[8] and gives water an unpleasant metallic taste and odor, an increased turbidity and a biofouling of pipelines.[2,9]

Manganese mainly affects on the brain and heart and can cause damage to the nervous system,[10] kidney, liver and cause mild anemia in low dose.[11] Several physicochemical methods for manganese elimination such as aeration, filtration , ion exchange, and settling techniques have evolved in search of efficiency, affordability, and ease of use.[12–14] During these last few years, the adsorption technique has been considered one of the most preferred methods for removing traces of heavy metals from water and wastewater due to its high efficiency, ease of handling and the availability of various adsorbents. This physicochemical process is a sustainable cost-effective alternative process in the environment.[15] A number of studies were carried out using differ-

ent adsorbents for manganese removal such as activated carbon,[1] moringa oleifera leaf, borassus flabellifer, mangifera indica,[16] pithecellobium dulce carbon,[7] palm fruit bunch, date stones or maize cobs.[17] Several parameters are important for comparing adsorbents such as local availability and the degree of treatment required, However, the cost parameter is rarely reported.[18] Plant materials, which are mainly composed of cellulosic materials, can adsorb micropollutants such as heavy metal cations in aqueous medium.[19,20] Several researches show that cellulose can be easily modified to obtain new adsorbent materials which are used for the adsorption of heavy metal ions and to improve its commercial value, making it eligible for new technological applications.[21] In the same context, Cactus cladodes from *Opuntia ficus indica* are primarily composed of water, carbohydrates (starch, cellulose, hemicellulose, pectin and chlorophyll), proteins, lignin, and lipids (carotene).[22,23] This composition allows *Opuntia ficus indica* to be used as an sorbent-coagulant. This study investigates heavy metals removal using cathodes powder. Preliminary results indicate low removal extents, less than 10 mg/g related to the very low specific surface area which is probably due to the covering of the majority of the surface by an excess of natural minerals, mainly $Ca(C_2O_4) \cdot H_2O$ (whewellite).[24] For performance improvement of this process, new by-products have been produced in the lab by modification of the surface of the natural *Opuntia ficus indica*.

The aim of this work is to develop a new adsorbent product following a valorization of a biomass, the activated *Opuntia ficus indica,* then to evaluate its properties of adsorption of manganese ions. The structures of the adsorbents as prepared (crude cactus and activated one) were identified by X-ray diffraction and infrared spectroscopy analysis. The influence of several parameters for manganese ions adsorption, such as pH, adsorbent dose, initial concentration, contact time and temperature were assessed. The adsorption equilibrium isotherm was fitted to Langmuir, Freundlich and Temkin models. The thermodynamic variables were calculated to verify the adsorption process. The adsorption kinetics process with the two adsorbents were analysed using the pseudo-first order, pseudo-second order, Elovich and intraparticle diffusion models. Different kinetic parameters, equilibrium adsorption capacities and correlation coefficients R^2 for each kinetic model were determined. The adsorption mechanism was elucidated for the activated adsorbent using IR spectroscopy and X-ray diffraction analysis.

2. Materials and Methods

2. 1. Materials and Reagents

The cladodes of *Opuntia ficus indica* were collected during July, in a plantation located in the region of Djebba in the north of Tunisia. All reagents were pure analytical grade and used as is without further purification. The chemicals used were hydrochloric acid, sodium hydroxide and $MnCl_2$, $4H_2O$ (Sigma-Aldrich, France).

2. 2. Methods

2. 2. 1. Preparation of *Opuntia Ficus Indica* Powder (OFIP)

Cladodes of *Opuntia ficus indica* were repeatedly washed with tap water to remove dust and extraneous material and then rinsed with distilled water. The pads were cut into small pieces of 1cm width to facilitate drying and followed by oven-drying at 333 K for 48 hours. The pads were then ground into a fine powder in the size range of 40 to 80 μm using a laboratory mill (Fisher Bioblock Scientific). Finally, the obtained adsorbent was stored in a clean and dry plastic vials for further use.

2. 2. 2. Synthesis of the Activated *Opuntia Ficus Indica* (Ac-OFIP)

The treatment of *Opuntia ficus indica* powder **OFIP** with a hydrochloric acid aqueous solution at a concentration of 1M was undertaken to ensure the removal of natural minerals excess such as whewellite and $CaCO_3$ from its surface. The suspension was stirred for about 4 hours until homogenized, after which the solution was filtered and washed with distilled water until the pH of the water became neutral. Finally, the chemically treated powder was dried overnight in an electric oven at 333 K, ground, stored in plastic containers. The adsorbents were named OFIP for the non-treated material and Ac-OFIP (activated *Opuntia ficus indica*) for the material treated with hydrochloric acid).

2. 2. 3. Characterization of OFIP and Ac-OFIP

All characterizations were carried out at the Materials and Environment Laboratory for Sustainable Development, LR18ES10. A powder X-ray diffractometer (Malvern PANalytical X'pert^3 Powder, Netherlands) was used to collect data, which works with a flat rotated sample holder and a 1 D-PIXcell detector.

The specific surface area of the materials based on the Brunauer–Emmett–Teller-theory (B.E.T measurements) were determined with a sorptometer (Micromeritics ASAP 2020, USA) using N_2 adsorption at 77 K.

The vibration properties as well as the chemical bonds present in the materials were analyzed by KBr pellet technique on a Bruker FT-IR spectrophotometer (Tensor 27, USA). Measurements were done within the range of 400–4000 cm^{-1}.

2. 2. 4. Chemical Analysis and Batch Adsorption Experiment

The manganese concentrations were determined by inductively coupled plasma optical emission spectrosco-

py ICP (ISO 11885: 2007) and results were expressed as mg/L. The solution pH was determined using a pH meter (BANTE Instruments). Batch adsorption experiments were carried out in conical flasks, with optimal values for adsorbent mass, pH, temperature and initial Mn (II) concentration. The flasks were then placed on an orbital laboratory shaker (Heidolph), at a constant speed of 100 rpm. Supernatant was collected and filtered through a Whatman filter paper before chemical analysis to remove the adsorbent materials particles that may be present in the supernatant.

2. 2. 5. Significance of Thermodynamic Parameters for the Adsorption Process

The adsorption capacity at equilibrium Qe (mg/g) of manganese by OFIP and Ac-OFIP was calculated using the following equation:

$$Qe = ((C_i - Ce) \times V/m) \quad (1)$$

where C_i and Ce are the solution manganese concentrations at the initial and at equilibrium (mg/L), V is the volume of the solution and m is the adsorbent mass added to the solutions (g).

The studies on the adsorption isotherm are of fundamental importance to determine the adsorption capacity of Mn (II) on the adsorbents and to develop an equation which accurately represents the results, and which could be used for the purposes of design. The models used in this process of fixing metal ions in solution on the two adsorbents are the Langmuir, the Freundlich and the Temkin equations.

The Langmuir isotherm involves adsorption on a single layer of the adsorbent and supposes three conditions: (a) the number of adsorption sites on the surface of the solid is fixed and the recovery of the surface of the solid in one molecular layer, (b) the enthalpy of adsorption is identical for each adsorption site and (c) no interaction between the adsorbed molecules.

The linear form of the Langmuir isotherm model can be expressed as:

$$\frac{Ce}{Qe} = \frac{1}{Q_{max} \times K_L} + \frac{Ce}{Q_{max}} \quad (2)$$

where Q_{max} (mg/g) is the monolayer saturation adsorption capacity and K_L (L/mg) is the Langmuir constant related to the adsorption capacity. The essential characteristics of the Langmuir isotherm can be expressed by a unitless constant called the separation factor (R_L) or equilibrium parameter, defined by Weber et al., as following:[25]

$$R_L = \frac{1}{1+K_L \times C_i} \quad (3)$$

with the K_L the Langmuir constant and C_i, initial concentration value. When $R_L > 1$, the isotherm is unfavorable and linear when equal to 1. It is favorable if $0 < R_L < 1$ and irreversible if it is equal to zero. Unlike Langmuir, who assumes that the enthalpy of adsorption of fluids on solids is a constant with respect to the recovery rate of the surface of the solid, Freundlich assumes a logarithmic variation of this enthalpy according to the rate of recovery. According to the logarithmic form of the Freundlich isotherm, when $R_L > 1$, the isotherm is unfavorable and when R_L is equal to 1, it is linear. It is favorable if $0 < R_L < 1$ and irreversible if R_L takes the value zero. The logarithmic form of the Freundlich isotherm is expressed as:

$$ln\, Qe = lnK_F + \frac{1}{n} ln\, Ce \quad (4)$$

K_F (mg/g) and n are Freundlich constants. The Temkin model is based on the fact that the heat of adsorption varies linearly with the degree of recovery; this variation can be related to the heterogeneity of the surface, or to lateral interactions between adsorbed molecules. The Temkin's relationship in linear form is expressed as follows:

$$Qe = B\, ln\, K_T + B\, ln\, Ce \quad (5)$$

B (J/mol), the Temkin constant relative to the heat of adsorption and K_T (L/g), the equilibrium adsorption constant corresponding to the maximum binding energy.

The variations of the standard enthalpy ΔH°, the standard entropy ΔS° and the Gibbs free energy ΔG° during the adsorption of manganese by OFIP and Ac-OFIP can be evaluated from the following equations:

$$\Delta G^\circ = -RT ln K_C \quad (6)$$

$$K_C = \frac{Qe}{Ce} \quad (7)$$

ΔG° is also linked to ΔH° and ΔS° by:

$$\Delta G^\circ = \Delta H^\circ - T\Delta S^\circ \quad (8)$$

R is the gas constant with a value of 8.314 J/mol K and T is the absolute temperature (K).

Substituting Eq. (6) into Eq. (8) gives:

$$ln\, K_C = -\frac{\Delta H^\circ}{RT} + \frac{\Delta S^\circ}{R} \quad (9)$$

The thermodynamic properties of an adsorption process are necessary to determine whether the process is favorable or not. They can also help to understand the binding mechanisms of metals on adsorbents and show whether the process follows physisorption or chemisorption.[26] In physisorption, the adsorbate (metal ion) is fixed to the surface of the solid (adsorbent) by weak Van der Waals attractions and by a low heat of adsorption of approximately 20 to 40 KJ/mol. Consequently, the process is rapid and reversible in nature.[27] However, the current study considers about chemisorption when chemical bonds form between the

surface of the solid (adsorbent) and the adsorbate (metal ion) and with high heat of adsorption (40–400 KJ/mol). In this case, it is difficult to remove the heavy metals adsorbed from the adsorbent; therefore, chemisorption is slow and irreversible in nature.[28]

Adsorption Kinetics Models

In order to investigate the mechanism of manganese adsorption on the two adsorbents (OFIP and Ac-OFIP), four kinetics models are studied: pseudo-first order, pseudo-second order, Elovich and intraparticle diffusion.

Pseudo-First Order

The Lagergren relation, based on the adsorbed quantity, is the first-rate equation established to describe the kinetics of sorption in a liquid – solid system. This pseudo-first order model is represented by the following relation:

$$ln(Qe - Q_t) = ln\,Qe - \frac{K_1\,t}{2.303} \quad (10)$$

where Qe (mg/g) is the quantity adsorbed at equilibrium, Q_t (mg/g) is the quantity adsorbed at the time of the adsorption process (t) and K_1 (min^{-1}) is the pseudo-first-order rate constant.

Pseudo-Second Order

The application of Blanchard's model, allows to describe the adsorption process as pseudo-second order reaction, represented by the following equation:

$$\frac{1}{Q_t} = \frac{1}{K_b \times Qe^2} + \frac{t}{Qe} \quad (11)$$

where Qe (mg/g) is the quantity adsorbed at equilibrium, Q_t (mg/g) is the quantity adsorbed at time t, t is the time of the adsorption process and k_b (mg/g.min) is the pseudo-second-order adsorption rate constant.

Elovich Equation

The Elovich model is one of the most useful for describing such activated chemical adsorption. It is often valid for systems in which the adsorption sites are heterogeneous. The Elovich equation is as follows:

$$Q_t = \frac{1}{b} ln(ab) + \frac{1}{b} ln\,t \quad (12$$

where Q_t (mg/g) is the quantity of adsorption at time t (min), a (mg/g) is an initial adsorption rate and b (g/mg) is the desorption constant.

Intraparticle Diffusion Model

The intraparticle diffusion model has widely been applied for the analysis of adsorption kinetics. This model is represented by the equation:

$$Q_t = k_i\,t^{0.5} + C \quad (13)$$

where Q_t is the quantity of adsorption (mg/g) at time t (min), k_i ($mg/g.min^{0.5}$) is an intraparticle diffusion rate constant and C is the intercept.

3. Results and Discussion

In this study, manganese adsorption onto OFIP and Ac-OFIP was investigated as a function of solution pH, adsorbent dosage, initial concentration of Mn (II) and temperature.

3. 1. Analysis of the biosorbents

3. 1. 1. XRD Characterization

The structure analysis of the *Opuntia ficus indica* powder by X-ray diffraction prior and after treatment (OFIP / Ac-OFIP) (Fig. 1) was performed to identify the crystalline and amorphous regions present in these samples. The X-ray pattern of OFIP powder shows strong crystalline peaks characteristic for calcium oxalate monohydrate (whewellite) at 14–15° and 24–25° (2θ), which was identified with the PDF # 20–0231 of ICDD-JCPDS database. This result is in agreement with that reported by Monje and Baran[29] and Contreras-Padilla et al.,[24] which identified the presence of calcium oxalate in different Cactaceae species belonging to the Opuntioideae subfamily, including *Opuntia ficus indica*. Furthermore, the results showed three Bragg reflections located at 29–30, 39–40 and 45–50° (2θ) in the pattern which are indicative of the presence of calcium carbonate $CaCO_3$ (PDF # 47-1743).

The x-ray pattern of Ac-OFIP powder (Fig. 1) is typical for cellulose I. The four well defined crystal peaks observed around 2θ = 15°, 16.5°, 22° and 35° are assigned to (1–10), (110), (200) and (004) respectively.[30] Unlike hemicellulose and lignin, which are amorphous in nature, cellulose has a crystal structure due to hydrogen bonding interactions and Van der Waals forces between adjacent molecules.[31] The crystallinity of the fibers of *Opuntia ficus indica* powder after treatment was well assessed. The treat-

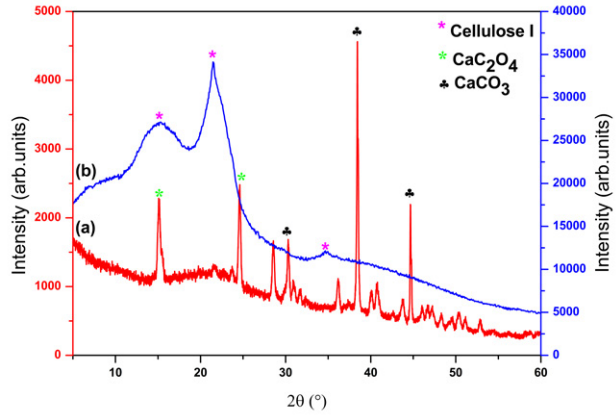

Fig. 1. XRD patterns of OFIP (a) and Ac-OFIP (b)

ment had effectively influenced the crystallinity of cellulose as reported by Mwaikambo and Ansell[32] stating that the alkaline chemical treatment on vegetable fibers increases their rigidity because the impurities present in them can be eliminated during this treatment. Therefore, the crystallinity of the Ac-OFIP powder can be determined and compared to the untreated OFIP powder to gain access to the effectiveness and importance of the activation process.

3. 1. 2. FT-IR Measurements

The spectra of OFIP and Ac-OFIP (Fig. 2) were investigated to obtain information on the nature of functional groups at the surface of the adsorbents. The infrared (IR) spectrum of OFIP showed broad, strong and superimposed bands in the 3600–3200 cm^{-1} region due to the elongation of the O-H bonds. The bands at 2928 cm^{-1}, 2858 cm^{-1} (different C-H vibrations), 1613.96 cm^{-1}, 1414.56 cm^{-1} and 780 cm^{-1} (different vibrations and deformation of the carboxylic groups) are characteristic of OFIP powder with the presence of calcium oxalate monohydrate (whewellite) and carbonates according to Contreras-Padilla et al.[24] Absorption peaks in the region of wavenumbers lower than 800 cm^{-1} could be attributed to N-containing bioligands as mentioned in the literature.[33] Due to OFIP's activation process with the acid treatment, a lot of FT-IR peaks have shifted in the Ac-OFIP spectrum. Thus, the intensity of the band linked to –OH (3600–3200 cm^{-1}) decreased after activation, which indicates that the treatment with acid leads to the breaking of weak bonds, and the band around between 1500–1750 cm^{-1} attributed to vibrations of carbonyl bonds C = O become more resolved and intense around 1740 cm^{-1}. The peaks at 1613.9 cm^{-1}, 1414.5 cm^{-1},780 cm^{-1} and near the region 800 cm^{-1} have completely disappeared in Ac-OFIP spectrum due to the elimination of calcium oxalate and carbonate and N-containing bioligands.

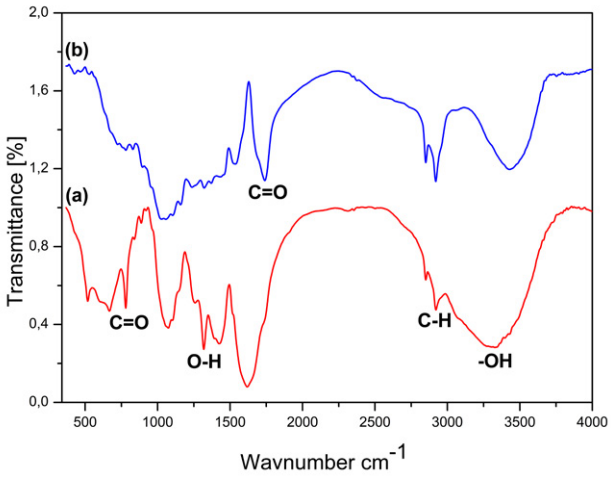

Fig. 2. FT-IR spectra of OFIP (a) and Ac-OFIP (b).

3. 1. 3. B.E.T Surface Areas

The specific surfaces of the two adsorbents Ac-OFIP and OFIP were determined by B.E.T and the values obtained indicate a very small specific surface for the untreated cactus powder. Barka et al. have already reported similar values in the range of 1.01 m^2/g in their study of the B.E.T surfaces of the Moroccan biosorbent *Opuntia ficus indica*.[33] They linked this result to the fact that the OFI can be considered as a non-porous material with no defined opening on their morphology and therefore without internal surface. The main reason could be the agglomeration of well-crystallized minerals ($CaCO_3$, CaC_2O_4 H_2O) on the surface of the cladodes, characterized by XRD measurement and IR spectroscopy[29] which contributes to the reduction of the porous surface and therefore to the specific surface. The OFIP product has a B.E.T surface area of 1.6 m^2/g and a porous volume equal to 0.002 cm^3/g, while Ac-OFIP has a significantly larger B.E.T surface area, 12.4 m^2/g and a porous volume equal to 0.090 cm^3/g. The increase in the B.E.T surface area of OFIP after treatment could be attributed to the removal of whewellite particles, carbonates and other impurities from OFIP. All these results confirmed the successful synthesis of Ac-OFIP.

3. 2. 1. Effect of pH

The pH of the aqueous solution is an important variable, which can have a significant effect on the extent of adsorption, because it influences on the surface properties of the adsorbent.[34–36] In addition, it influences the ionization degree of metals in the solution.[37–39] Manganese adsorption onto OFIP and Ac-OFIP was investigated at initial pH range of 4–8 and the results are shown in Fig. 3. All the other factors were kept constant that is: temperature at 298 K, adsorbent dosage at 0.4 g/L, contact time of 24 h, agitation speed kept at 100 rpm and Mn (II) initial concentration of 27.75 mg/L. As shown in Fig. 3 the percentage removal of Mn (II) greatly depends on pH for the Ac-OFIP powder. Firstly, the percentage removal was found to increase gradually with the increase of pH up to 5 for the OFIP with no considerable change after the pH 5. Secondly, for the adsorbent treated Ac-OFIP, the percentage removal of Mn (II) ion increased with an increase in the pH from 4 to 7 and it was almost constant up to pH 8. The results of the percentage of maximum elimination of the manganese ions were of the order of 35.5% and 91.6% for OFIP and Ac-OFIP, respectively. The small metal adsorption at low pH values could be attributed to the competition of hydrogen ions with the manganese for the occupancy of the adsorption sites. Indeed, at low pH values a protonation of functional groups was produced on the adsorbent surface which limited the interaction between the positively charged metal ions and the two adsorbents due to repulsive forces; this reduced the Mn (II) adsorption capacity.

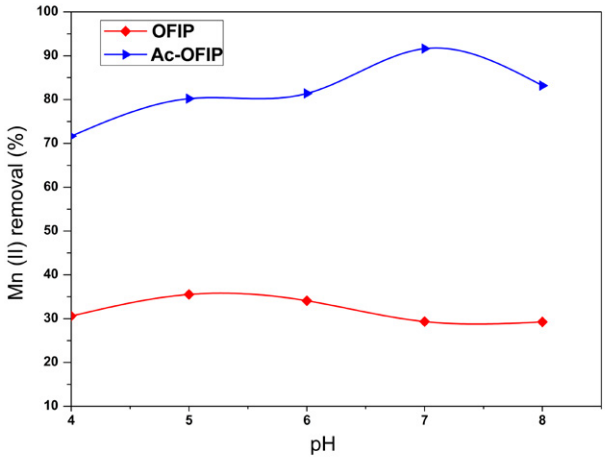

Fig. 3. Effect of pH on the adsorption of Mn (II) ions on OFIP and Ac-OFIP.

There was a significant increase in the removal of metal ions at pH 5 for OFIP and 7 for Ac-OFIP, this can be explained by the fact that the adsorption sites were no longer affected by the pH variation. At a higher pH, the removal efficiency of Mn (II) ions gradually decreased with the two adsorbents. A pH greater than 8 has been neglected due to the precipitation of $Mn(OH)_2$ which could be formed with the increasing amount of OH^- in the solution, which would be mistaken as adsorption due to the different powders. For subsequent investigations, pH 5 and 7 appeared as the optimal conditions for OFIP and Ac-OFIP respectively.

3. 2. 2. Effect of Adsorbents Dosage

The dependence of manganese adsorption on dose was studied at pH 5 for OFIP and pH 7 for Ac-OFIP. The initial concentration of Mn (II) was fixed at 27.75 mg/L and contact time at 24 h. All experiments were carried at ambient temperature with adsorbent concentrations from 0.2 g/L to 1.3 g/L. The relationship between the percentage removal of Mn (II) and the dose of OFIP and Ac-OFIP is shown in Fig. 4. The curves obtained show a great capacity of the Ac-OFIP material in the elimination of Mn (II) ions, which can reach approximately 99.6%, while it only reaches 52% for OFIP. The results obtained also indicate that the rate of removal of Mn (II) ions increases with the amounts of adsorbent in the solution to reach its maximum at optimal dosages of 0.7 g/L for Ac-OFIP and 1.1g/L for OFIP. This trend in uptake is attributed to the increasing number of negatively charged active sites and surface area for Mn (II) binding on the adsorbent. After the optimum dosage, the elimination rate does not change, which corresponds to the saturation of different types of adsorbent active sites by the adsorbate (ions of metals Mn (II) in the system).

3. 2. 3. Effect of Mn (II) Initial Concentration

In order to evaluate the effect of Mn (II) ion concentration on the adsorption behavior of the two adsorbents (OFIP and Ac-OFIP), adsorption experiments with varying manganese concentrations of 2 mg/L to 85 mg/L were studied in the best experimental conditions: pH 5.0 for OFIP, pH 7.0 for Ac-OFIP and adsorbent concentration of 0.7g/L for Ac-OFIP, and 1.1 g/ L for OFIP. Fig. 5 shows that the highest percentage removal of Mn (II) are observed for Ac-OFIP (99.99%) with a maximum adsorption capacity of 42.02 mg/g. However, pure OFIP exhibits a low adsorption capacity of only 20.8 mg/g. It can also be deduced from the results presented in Fig. 5 that for the two adsorbents, the maximum adsorption capacities are only reached for low initial concentrations of Mn (II), then the elimination values decrease with increasing initial concentration of the manganese solution. This is due to the fact that some manganese ions remained in the solution due to

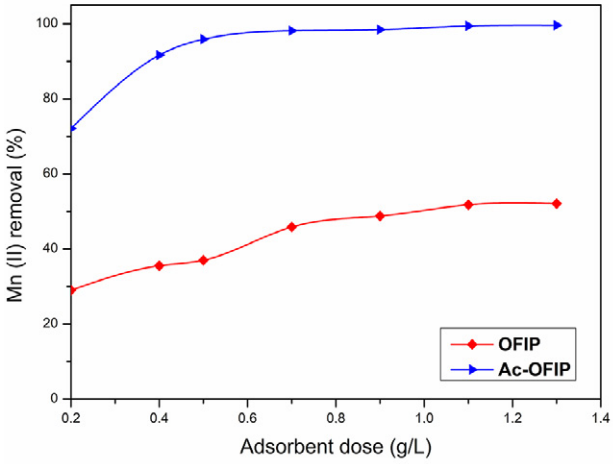

Fig. 4. Effect of adsorbent dose on the elimination of Mn (II) ions for OFIP and Ac-OFIP.

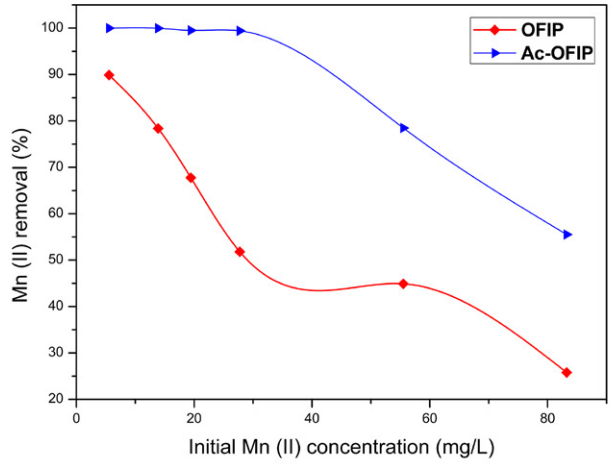

Fig. 5. Effect of Mn (II) concentration on removal rate for OFIP and Ac-OFIP.

Table 1. Fitting parameters and goodness of fit for three different isotherm models (Langmuir, Freundlich and Temkin) applied to experimental adsorption data.

Adsorbents	Langmuir			Freundlich			Temkin		
	Q_{max} (mg/g)	K_L	R^2	n	K_F	R^2	B	K_T	R^2
OFIP	20.8	0.245	0.99	3.244	6.157	0.95	3.306	6.36	0.96
Ac-OFIP	42.02	6.102	0.99	5.437	25.84	0.90	3.563	8.32	0.98

the saturation of the active sites on the adsorption surface of the adsorbent materials and thus sites with high affinity were the first to be saturated. Subsequently, the affinity of the metal cations for the remaining sites decreased.

3. 2. 4. Effect of Temperature

The temperature of the medium is a very important parameter in this process because it exerts a considerable influence on the adsorption rate.[40] The temperatures used in this experimental phase vary from 293 to 313 K with an interval of 5 K. The results of the tests carried out show that the temperature acts directly on this adsorption process with maximum fixation at 308 K for the two adsorbents. This is explained by the fact that the adsorption of manganese in aqueous medium by OFIP and Ac-OFIP is exothermic. The percentage removal of Mn (II) for this medium are 80% and 36% for Ac-OFIP and OFIP, respectively, (Fig. 6).

3. 2. 5 Effect of Contact Time

The effect of contact time on the percent removal of Mn (II) by OFIP and Ac-OFIP was studied in the range 10–120 min to find equilibrium time for adsorption (Fig. 7). The adsorption experiments were carried out at optimal experimental conditions: pH 5.0 in the case of OFIP as adsorbent with concentration of 1.1 g/L and pH 7.0 for the case of Ac-OFIP as adsorbent with concentration of 0.7 g/L. The initial concentration of manganese was 20 mg/L in both cases. As shown in Fig. 7 the percentage removal of Mn (II) with both adsorbents (OFIP and Ac-OFIP) is higher at the beginning. This is probably due to the fact that at the beginning a larger surface of adsorbent is available for the adsorption of Mn (II). The equilibrium was reached within the first 60 and 80 minutes of stirring with Ac-OFIP and OFIP, respectively. Beyond this time, we noticed it reached a saturation level. As the contact time increased the active surface adsorption sites on both adsorbents were filled.

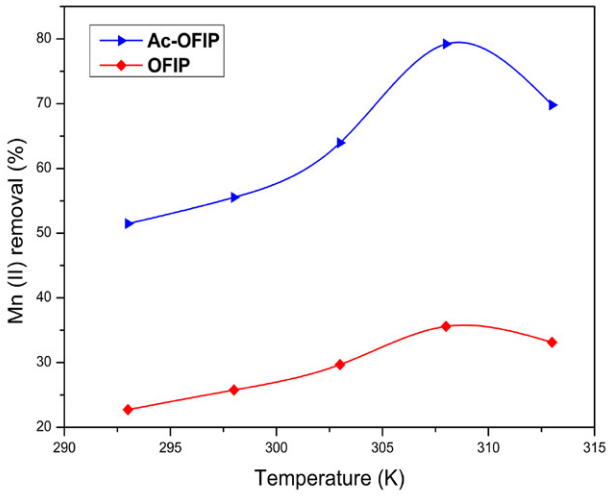

Fig. 6. Effect of temperature on removal rate for OFIP and Ac-OFIP.

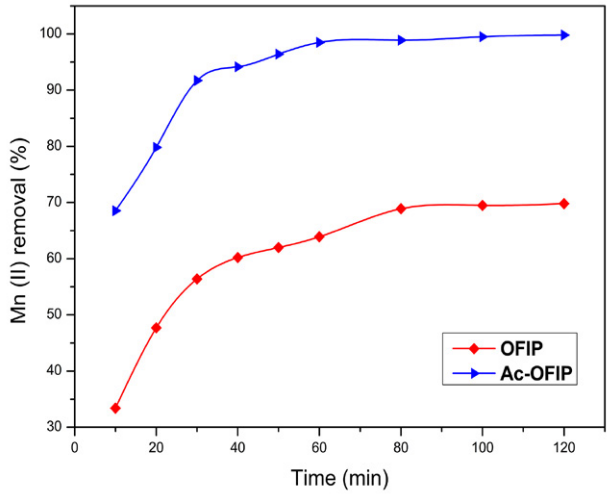

Fig. 7. Effect of contact on removal rate for OFIP and Ac-OFIP.

3. 3. Adsorption Isotherms

The application of Langmuir, Freundlich and of Temkin models on the results of the experiments was undertaken under the current study operating conditions (Vag: 100 rpm; T_{milieu}: 298 K; pH milieu: 5 with OFIP, 7 with Ac-OFIP; and $m_{(OFIPand\ Ac\text{-}OFIP)}$: 1.1g/L and 0.7 g/L). Fig. 8 (a) and Fig. 9 (a) demonstrate the linear plot of Ce/Qe as a function of Ce for OFIP and Ac-OFIP respectively. The values of Q_{max} and K_L were determined from slope and the ordinate at the origin of the linear regressions as shown in Table 1. The R_L values calculated for this study are illustrated in Table 2. Two plots of ln (Qe) as a function of ln (Ce) are shown in Fig. 8 (b) and Fig. 9 (b) for OFIP and Ac-OFIP, respectively, where the values of K_F, n and the correlation coefficient R^2 for the Freundlich model are given in Table 1.

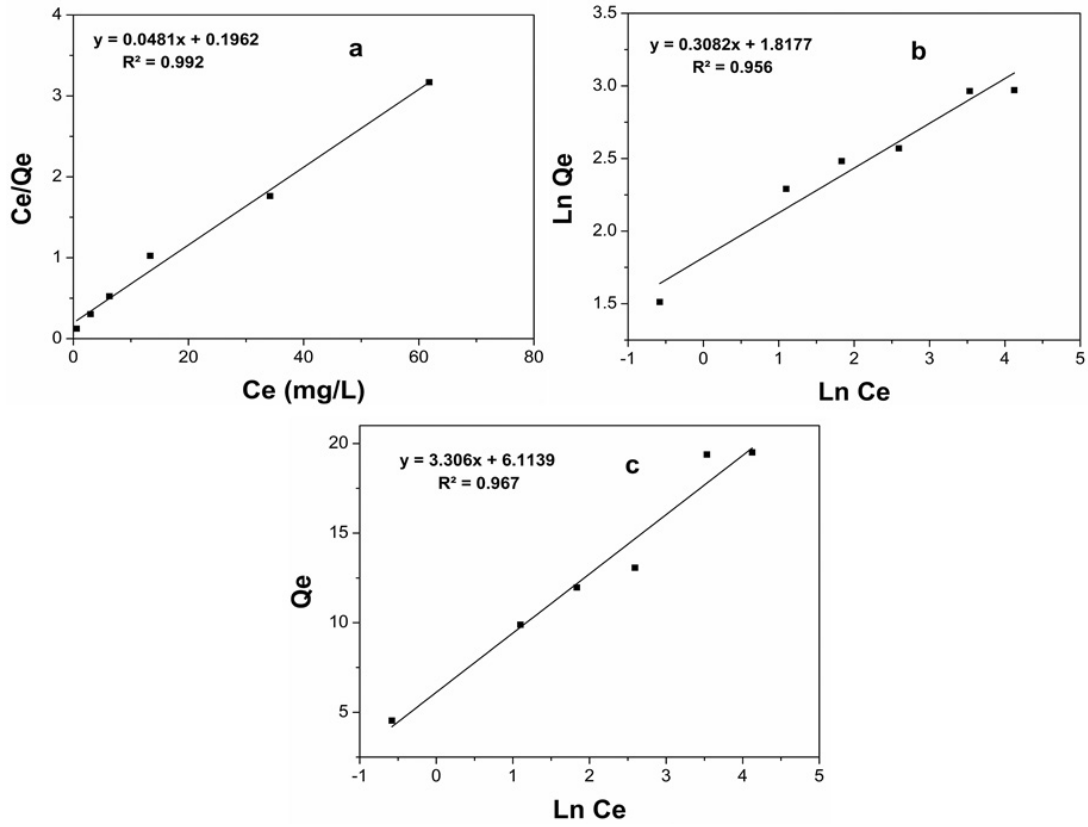

Fig. 8. Langmuir isotherm (a), Freundlich isotherm (b) and Temkin isotherm (c) for Mn (II) adsorption on OFIP adsorbent.

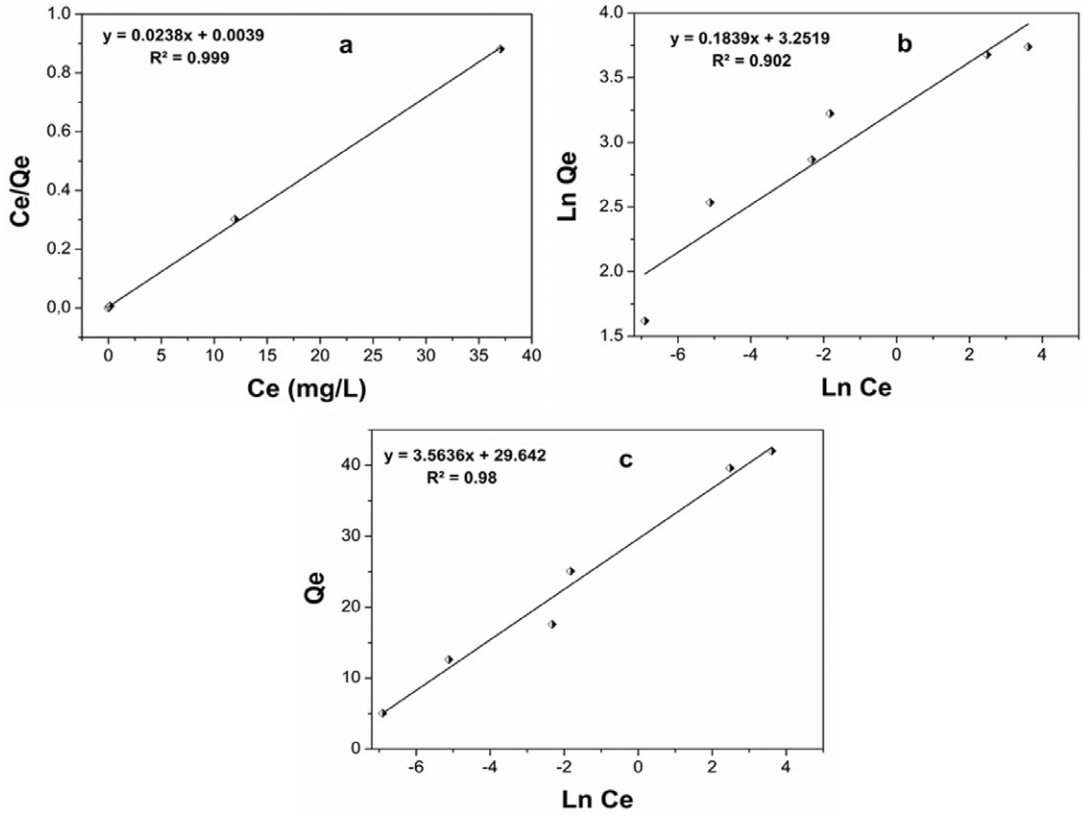

Fig. 9. Langmuir isotherm (a), Freundlich isotherm (b) and Temkin isotherm (c) for Mn (II) adsorption on Ac-OFIP adsorbent.

Table 2. R_L as a function of the initial concentration of manganese

C_i (mg/L)	5.55	13.87	19.42	27.75	55.50	83.25
R_L (OFIP)	0.424	0.227	0.173	0.128	0.068	0.046
R_L (Ac-OFIP)	0.028	0.011	0.008	0.005	0.002	0.001

Table 3. Values of thermodynamic parameters of manganese adsorption at different temperatures by OFIP and Ac-OFIP.

Adsorbent	Temperature K	K_F	ΔG° KJ/mol	ΔH° KJ/mol	ΔS° KJ/mol K
OFIP	293	0.2262	3.6210		
	298	0.2670	3.2717	26.30	0.077
	303	0.3248	2.8330		
	308	0.4248	2.1925		
	313	0.3807	2.5128		
Ac-OFIP	293	0.8158	0.4958		
	298	0.9605	0.0998	54.79	0.183
	303	1.3654	−0.7845		
	308	2.9303	−2.7530		
	313	1.7770	−1.4961		

Figures 8 (c) and 9 (c) show plots of Qe as a function of ln (Ce), which permitted to determine the isothermal constants K_T and B. The values of K_T, B and the correlation coefficient R^2 for Temkin model are given in Table 1.

The best data adjustments were obtained with the Langmuir isothermal model for the OFIP and Ac-OFIP. This observation is justified by the values of the regression coefficients which are better for the OFIP and Ac-OFIP with the Langmuir equation (R^2 Langmuir: 0.99). It is clear

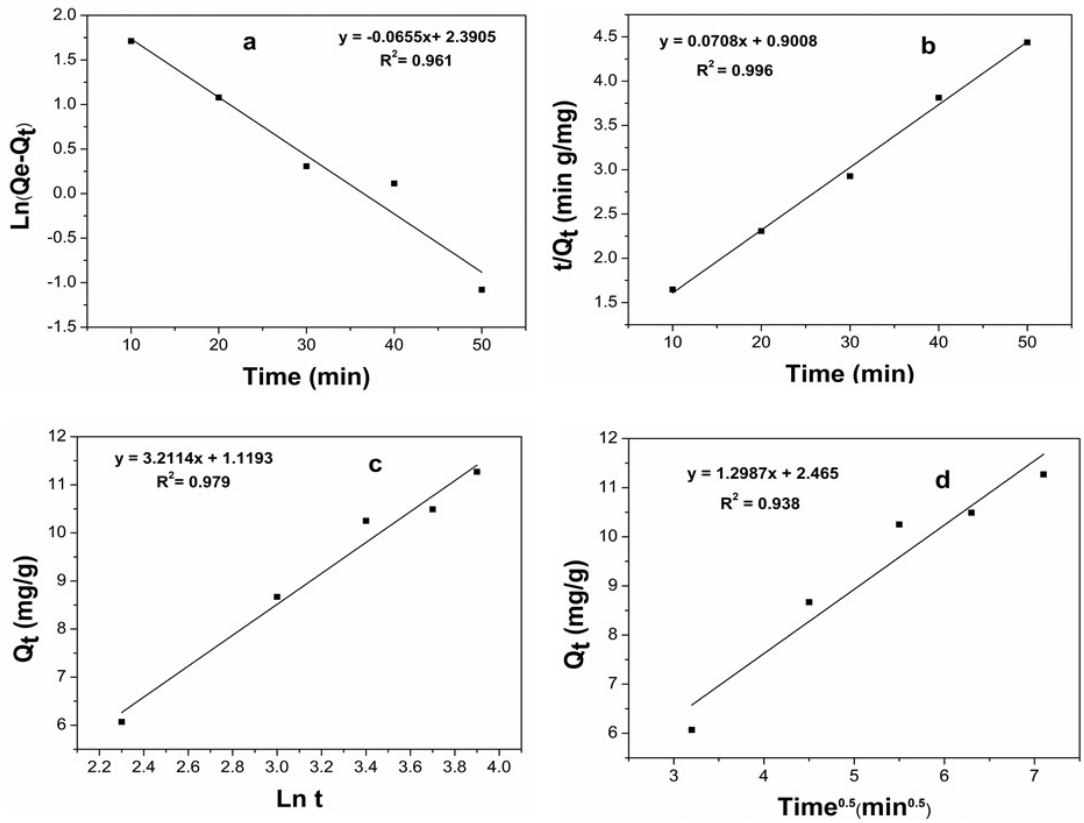

Fig. 10. Pseudo-first-order (a), pseudo-second-order (b), Elovich (c) and intraparticle diffusion (d) models for Mn (II) adsorption on OFIP adsorbent.

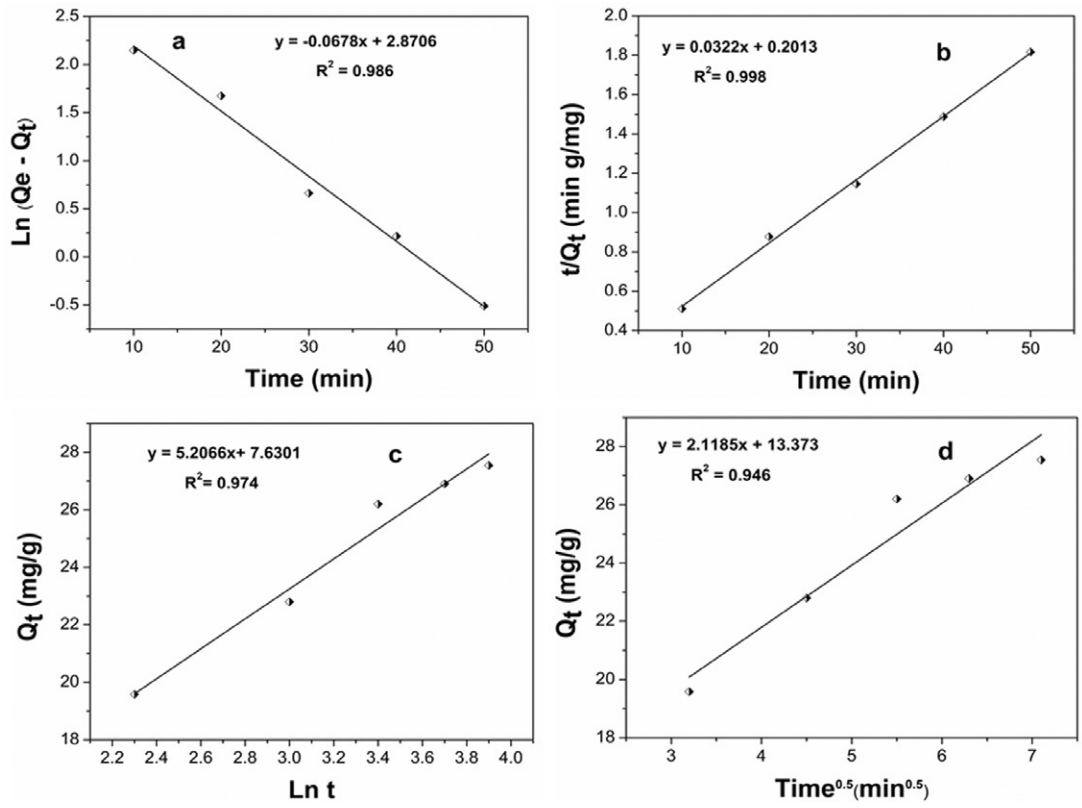

Fig. 11. Pseudo-first-order (a), pseudo-second-order (b), Elovich (c) and intraparticle diffusion (d) models for Mn (II) adsorption on Ac-OFIP adsorbent.

from Table 2 that the value of the R_L ratio decreases with the increase of the initial concentration for the two cases of adsorbents and remain between 0 and 1 suggesting a favorable significance for the Langmuir model.

3. 4. Thermodynamics Studies

The estimated thermodynamic parameters ΔH°, ΔS° and ΔG° of the effect of the temperature on the adsorption of Mn (II) by pure and modified *Opuntia ficus indica* (OFIP/Ac-OFIP) are given in the Table 3.

All the values of free energies for the chosen temperature range (ΔG° > 0) revealed that the adsorption of Mn (II) by OFIP was not a spontaneous process, whereas for the adsorption of Mn (II) by Ac-OFIP, the free energy values showed positive rates at low temperatures and tended towards the spontaneity of the adsorption process with increasing temperature. The adsorption of Mn (II) increased as the temperature increased in the range of 293 to 313 K, which implies that the process is more favorable at high temperatures.

A linear plot of ln K_F against 1/T in the temperature range of 293 to 308 K was established and ΔH° and ΔS° were determined.

The calculated enthalpy values are greater than zero (ΔH° > 0) and have been found to be 26.30 and 54.79 kJ/mol respectively for OFIP and Ac-OFIP, which shows that this adsorption process is endothermic in nature. The enthalpy value ΔH° is less than 40 kJ/mol for OFIP, which indicates that physisorption is the main adsorption mechanism, while it is greater than 40 kJ/mol for Ac-OFIP and this indicates in this case that chemisorption is the main mechanism of adsorption. The positive entropy values for the two adsorbents (ΔS° > 0) reflect a disorder in the system at the solid solution interface that occurred during adsorption.

3. 5. Adsorption Kinetics

Details of the application of the four kinetic models (pseudo-first order, pseudo-second order, Elovich and intraparticle diffusion). The results obtained from the experiments under optimum conditions are illustrated on Fig. 10 (a, b, c, d) and Fig. 11 (a, b, c, d). The linear plot of ln (Q_e-Q_t) versus of time t for OFIP and Ac-OFIP, respectively, is shown Fig. 10 (a) and Fig. 11 (b). The values of k_1, Q_e and R^2 were determined from slope and the ordinate at the origin of the linear regressions (Table 4).

Two plots of t/Q_t as a function of time t have been shown in Fig. 10 (b) and 11 (b) for OFIP and Ac-OFIP respectively, where the values of k_2, Q_e and the correlation coefficient R^2 for the pseudo-second order model are given in Table 4. Figures 10 (c) and 11 (c) show plots of Q_t as a function of ln t, which allowed to determine the constants

Table 4. Correlation coefficients R^2 and constant values of kinetics parameters of manganese adsorption by OFIP and Ac-OFIP.

Adsorbent	Pseudo-First-r Orde		Pseudo-Second-Order		Elovich Model		Intraparticle Diffusion	
OFIP	R^2	0.961	R^2	0.996	R^2	0.979	R^2	0.938
	$Q_{e\ (The)}$	11.61	$Q_{e\ (The)}$	11.61	a	4.553	k_i	1,298
	$Q_{e\ (Exp)}$	10.92	$Q_{e\ (Exp)}$	14.12	b	0.311	C	2,465
	K_1	0.150	K_2	0.006				
Ac-OFIP	R^2	0.986	R^2	0.998	R^2	0.974	R^2	0.946
	$Q_{e\ (The)}$	28.14	$Q_{e\ (The)}$	28.14	a	22.536	k_i	2.118
	$Q_{e\ (Exp)}$	17.65	$Q_{e\ (Exp)}$	31.06	b	0.192	C	13.373
	K_1	0.156	K_2	0.005				

a and b. The values of a, b and the correlation coefficient R^2 for Elovich model are given in Table 4. Figures 10 (d) and 11 (d) show the linear plot of Q_t as a function $t^{0.5}$ for OFIP and Ac-OFIP respectively, where the values of k_i and the correlation coefficient R^2 for the intraparticle diffusion model are given in Table 4.

As can be seen from the Fig. 10 and Fig. 11, the extremely high correlation coefficients R^2 for OFIP (0.996) and Ac-OFIP (0.998) were obtained for pseudo-second order model. Thus, adsorption of manganese onto adsorbents (OFIP and Ac- OFIP) followed the pseudo-second order kinetic process. In addition, equilibrium adsorption capacity values Qe calculated were in good agreement with experimental values for the two adsorbents.

3. 6. Adsorption Mechanisms of Mn (II)

3. 6. 1. XRD Analysis

Fig. 12 shows the XRD patterns of Ac-OFIP before and after the adsorption of Mn (II) ions. X-ray diffraction analysis was used to confirm the presence of Mn on the surface of the OFIP modified. Thanks to the appearance of new MnO_x peaks, it is possible to probe their presence. As mentioned in the previous sections, the adsorption of Mn (II) by Ac-OFIP is a chemisorption and a detailed inspection of the XRD diagram after the adsorption process could provide more information on the mechanism of adsorption. Compared to that of the pure Ac-OFIP pattern, new distinct peaks were observed on the Ac-OIFP diagram at 26.8°, 29.5° and 31.9° 2θ attributed to the typical peaks of MnO_x oxides according to references from PDF-4 database (ICDD). No strong evolution of the XRD diagram was noted, the Bragg angles of the cellulosic diagram (diffraction peaks) remained essentially unchanged following the adsorption process of the Mn (II) cations. These results suggest that the grafting of different MnO_x took place on the surface of the cellulose fibers, and the cellulose maintained its crystal structure. These results suggest that the Mn (II) adsorbed was first oxidized to higher degrees, and then, probably maintained on the surface of the adsorbent with different C-O-MnO_x bonds.

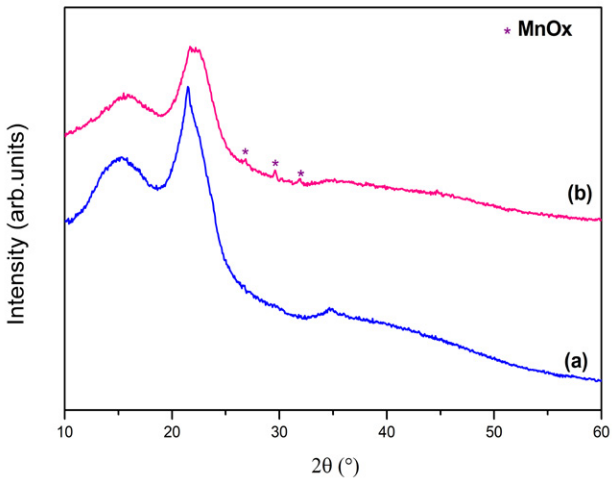

Fig. 12. Comparison in XRD patterns of Ac-OFIP (a) and Mn-Ac-OFIP (b).

3. 6. 2. Analysis of FT-IR Spectra

FT-IR spectra were also useful for judging the bonding states between functional groups of the adsorbent and the metal ion. The comparison of the IR spectra of pure Ac-OFIP and that after adsorption is well illustrated in Fig. 13. The appearance of an intense band at 620 cm^{-1} and three minor bands at 437cm^{-1}, 536 cm^{-1} and 474 cm^{-1} demonstrated the presence of different oxides of MnO_x on the adsorbent. In addition, the absorption bands of MnO_x, in the region of low frequencies were very broad; this was related to the crystalline and amorphous content and to the effect of the particle size on the spectral characteristics. Due to the interaction of the functional groups of the adsorbent with the Mn (II), FT-IR peaks can move towards lower or higher wavenumbers after the loading of Mn (II), depending on bond strength between metal ions and adsorbent.[41] It can be deduced from Figure 10 that after the adsorption of Mn (II), there was a change in the peak of the carbonyl group C = O from 1737 cm^{-1} to 1637 cm^{-1}, which may indicate that the carbonyl group is involved in the adsorption process.

Furthermore, the appearance of a broad band at 2130 cm^{-1} related to the carbonyl stretches for $Mn(CO)_n$ on the surface after adsorption, indicates the important role that it plays in the chemisorption of Mn (II) on ligands. On surfaces, the geometric arrangement of the CO bond can be determined from the vibration frequency.[42,43] The stretching of the free molecule C-O generally occurs at 2143 cm^{-1},[42,44] far from most other molecular vibrations, it provides a practical and sensitive indicator of binding interactions. In "classic" carbonyls, the stretching frequency C-O(ν_{CO}) is lowered compared to its value in the free CO molecule due to a marked decrease in bonding electron density and an increase in antibonding electron density in the π*.

The majority of the transition metal carbonyl complexes exhibit a red shift resulting in stretching of the carbonyl. In our case the charge-induced reduction in π back-bonding leads to a decreased red-shift in $Mn(CO)_n$ (υ_{CO} = 2130 cm^{-1}).

No change in the frequency of the cellulosic bands was noted following the adsorption process, suggesting that chemisorption took place on the surface of the cellulosic fiber, and also that Ac-OFIP continued to maintain its crystal structure.

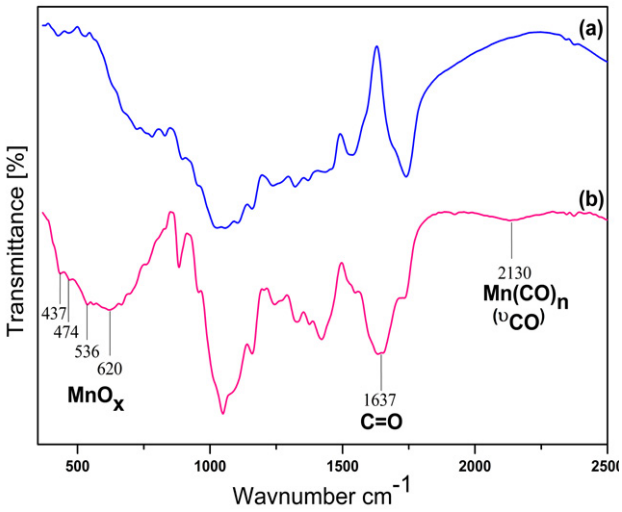

Fig. 13. Comparison in FT-IR spectra of Ac-OFIP (a) and Mn-Ac-OFIP (b).

3. 7. Comparison with the Other Adsorbents

Some adsorbents used for the removal of Mn (II) reported in the literature were compared with OFIP, and with Ac-OFIP as indicated in Table 5. The values obtained for the maximum adsorption capacity in this study are much higher compared to those obtained with other adsorbents (except the two studies 45 and 46). Therefore, it should be emphasized that OFIP and Ac-OFIP adsorbents can become a material of choice successfully compete with other absorbents.

Table 5. Comparison of maximum Mn (II) adsorption capacities with other adsorbents.

Adsorbents	Capacity (mg/g)	Reference
Ac-OFIP	42.0	This study
OFIP	19.5	This study
Pecan nutshell	103.8	45
Crab shell particles	69.9	46
Natural zeolitic tuff	10.0	47
Black carrot residues	5.2	48
Activated carbon immobilized Bytannic acid	1.7	49
Kaolinite	0.4	50
Pithacelobium dulce carbon	0.4	7

4. Conclusion

In this study, *Opuntia ficus indica* powder with and without activation treatment (OFIP, Ac-OFIP) have been used as an adsorbent in the removal of Mn (II) from aqueous solutions. The surface modifications of OFIP have been made to improve the selectivity of the by-products and thus have more affinity for the cations and improve the adsorption capacity. A very high percentage of manganese elimination has been observed in the case of Ac-OFIP. In the study of factors affecting the adsorption process, the percentage removal of Mn (II) increased with the pH and the dose of adsorbents up to the optimum values and there have been no considerable changes thereafter. The equilibrium absorption of the adsorbents has been found to decrease with the increase in the initial concentration of manganese ions in solution. The thermodynamic study has shown that this process is endothermic in nature and with a positive change in entropy for the two adsorbents, suggesting the affinity of the metal ion for the adsorbents. Chemisorption is the main adsorption mechanism for Ac-OFIP while it is physisorption for OFIP. A study of experimental isotherms such as Langmuir, Freundlich and Temkin revealed that the best fit has been obtained by the Langmuir model for OFIP and Ac-OFIP. The kinetic data is in good agreement with pseudo-second order kinetic model with high correlation coefficients for the two adsorbents. For Ac-OFIP, the XRD and infrared characterizations have confirmed that the process is chemisorption as suggested by the thermodynamic study. The adsorption mechanisms consisted of electrostatic interaction, oxidation of the Mn (II) adsorbed to higher degrees and then probably maintained on the surface of the adsorbent with different C-O-MnO_x bonds. The results have shown that Ac-OFIP is an effective adsorbent of Mn (II) which needs to be further explored.

Acknowledgements

Financial support from the Ministry of Higher Education and Scientific Research of Tunisia is gratefully ac-

knowledged. The authors appreciate Ms. Hajer REBAI for linguistic editing and proofreading of the manuscript.

Declaration of Interest Statement

We declare that we do not have any commercial or associative interest that represents a conflict of interest in connection with the work submitted.

5. References

1. A. Omri, M. Benzina, *Alex. Eng. J.* **2012**, *51*, 343–350. **DOI:**10.1016/j.aej.2012.06.003
2. H. A. Aziz, P. G. Smith, *Wat. Res.* **1996**, *30*, 489–492. **DOI:**10.1016/0043-1354(95)00178-6
3. D. L. Jensen, J. k. Boddum, S. Redemann, T. H. Christensen, *Environ. Sci. Technol.* **1998**, *32*, 2657–2664. **DOI:**10.1021/es9711270
4. G. R. Watzlaf, *Proceedings America Society of Mining and Reclamation*, **1987**, *17*, 83–90. **DOI:**10.21000/JASMR88010083
5. UNEP, North America's Environment, A thirty-years State of the Environment and Policy Retrospective, UNEP, New York, **2002.**
6. S. R. Taffarel, J. Rubio, *Miner. Eng.* **2010,** *23*, 1131–1138. **DOI:**10.1016/j.mineng.2010.07.007
7. K. A. Emmanuel, A. Veerabhadra Rao, *Rasayan J. Chem.* **2008**, *1*, 840–852.
8. B. Kwakye-Awuah, B. Sefa-Ntiri, E. Von-Kiti, I. Nkrumah, C. Williams, *Water J.* **2019**, *11*,1–19. **DOI:**10.3390/w11091912
9. K. Z. Al-Wakeel, H. A. Abd-El Monem, M. M. H. Khalil, *Chem. Eng. J.*, **2015**, *3*, 179–186. **DOI:**10.1016/j.jece.2014.11.022
10. M. Aschner, K. M. Erikson, E. H. Hernández, R. Tjalkens, *Neuromolecular Med.* **2009**, *11*, 252–266. **DOI:**10.1007/s12017-009-8083-0
11. A. Abdul kadir, N. Othman, N. A. Azmi, *IJSCET*. **2012**, *3*, 2180–3242.
12. WHO, Guidelines for drinking-water quality, 2nd ed. WHO Press Geneva Switzerland, **2011**, 1–21.
13. J. B. Awuah, N. Dzade, R. Tia, E. Adei, B. Kwakye-Awuah, R. R. A. Catlow, N. H. De Leeuw, *Phys. Chem. Chem. Phys.* **2016**, *18*, 11297–11305. **DOI:**10.1039/C6CP00190D
14. M. Ahmad, Iron and Manganese removal from ground water: geochemical modeling of the vyredox method. Master Thesis, University of Oslo, Oslo, Norway, **2012**.
15. P. Marzal, A. Seco, C. Gabaldo, J. Ferrer, *J. Chem. Technol. Biotechnol.*, **1996**, *66*, 279–285. **DOI:**10.1002/(SICI)1097-4660(199607)66:3<279::AID-JCTB506>3.0.CO;2-K
16. A. Saranya, S. Sasikala, G. Muthuraman, *Int. J. Recent Sci. Res.* **2017**, *8*, 17867–17876.
17. M. M. Nassar, K. T. Ewida, E.E. Ebrahiem, Y. Magdy, M. H. Mheaedi, *Adsorpt. Sci. Technol.* **2004**, *22*, 25–37. **DOI:**10.1260/026361704323150971
18. S. E. Bailey, T. J. Olin, R.M. Bricka, D. D. Adrian, *Water Res.* **1999**, 33, 2469–2479. **DOI:**10.1016/S0043-1354(98)00475-8
19. G. Sun, W. Shi, *Ind. Eng. Chem. Res.***1998**, *37*, 1324–1328. **DOI:**10.1021/ie970468j
20. W. Zhang, H. Duo, S. Li, Y. An, Z. Chen, Z. Liu, Y. Ren, S. Wang, X. Zhang, X. Wang, *Colloids Interface Sci. Commun.* **2020,** *38,* 1–13. **DOI:**10.1016/j.colcom.2020.100308
21. A. Negrea, A. Gabor, C. M. Davidescu, M. Ciopec, P. Negrea, N. Duteanu, A. Barbulescu, *Sci. Rep.* **2018**, *8*, 1–11. **DOI:**10.1038/s41598-017-18623-0
22. M. A. Ayadi, W. Abdel maksoud, M. Ennouri, H. Attia, *Ind. Crop. Prod.* **2009**, *30*, 40–47. **DOI:**10.1016/j.indcrop.2009.01.003
23. G. Lassoued Ben Miled, B. Djobbi, R. Ben Hassen, *J. Water Chem. Techno.* **2018**, *40*, 285–290. **DOI:**10.3103/S1063455X18050065
24. M. Contreras-Padilla, E.M. Rivera-Muñoz, E. Gutiérrez-Cortez, A. Del Real, M.E. Rodríguez-García, *J. Biol. Phys.* **2015**, *41*, 99 –112. **DOI:**10.1007/s10867-014-9368-6
25. T. W. Weber, R. K. Chakravorti, *AIChE J.* **1974**, *20*, 228–238. **DOI:**10.1002/aic.690200204
26. M. N. Sahmoune, *Chem. Eng. Technol.* **2016**, *39***,** 1617–1628. **DOI:**10.1002/ceat.201500541
27. M. T. Yagub, T. K. Sen, S. Afroze, H. M. Ang, *Adv. Colloid. Interfac.*, **2014**, *209*, 172–184. **DOI:**10.1016/j.cis.2014.04.002
28. O. Aksakal, H. Ucun, *J. Hazard. Mater.* **2010**, *181*, 666–672. **DOI:**10.1016/j.jhazmat.2010.05.064
29. P. Monje, E. Baran, *J. Plant Physiol.*, **2004**, *161*, 121–123. **DOI:**10.1078/0176-1617-01049
30. D. Klemm, B. Heublein, H. P. Fink, A. Bohn, *Angew. Chem. Int. Ed.* **2005**, *44*, 3358–3393. **DOI:**10.1002/anie.200460587
31. Y. H. Zhang, L. R. Lynd, *Biotechnol. Bioeng.* **2004**, *88*, 797–824. **DOI:**10.1002/bit.20282
32. L. Y. Mwaikambo, M. P. Ansell, *J. Mater. Sci.* **2006**, *41*, 2483–2496. **DOI:**10.1007/s10853-006-5098-x
33. N. Barka, K. Ouzaouit, M. Abdennouri, M. El Makhfouk, *J. Taiwan Inst. Chem. E.* **2013**, *44***,** 52–60. **DOI:**10.1016/j.jtice.2012.09.007
34. A. F. Baybars, M. Korkmaz, C. Özmetin, *J. Disper. Sci. Technol.* **2016,** *37*, 991–1001. **DOI:**10.1080/01932691.2015.1077455
35. D. P. Tiwari, D. K. Singh, D. N. Saksena, *J. Environ. Eng.* **1995**, *121*, 479 – 481. **DOI:**10.1061/(ASCE)0733-9372(1995)121:6(479)
36. H. A. Elliot, C. P. Huang, *Water Res.*, **1981**, *15*, 849 – 855. **DOI:**10.1016/0043-1354(81)90139-1
37. Q. Du, Z. Sun, W. Forsling, H. Tang, *J. Colloid. Interf. Sci.* **1997**, *187*, 232–242. **DOI:**10.1006/jcis.1996.4676
38. K. S. Hui, C. Y. H. Chao, S. C. Kot, *J. Hazard. Mater.* **2005**, *127*, 89–101. **DOI:**10.1016/j.jhazmat.2005.06.027
39. M. Fadel, M. N. Hassanein, M. M. Elshafei, A. H. Mostafa, M. A. Ahmed, H. M. Khater, *HBRC.* **2017**, *13*, 106–113. **DOI:**10.1016/j.hbrcj.2014.12.006
40. K. P Yadava, B. S. Tyagi, V.N. Singh, *Environ. Technol. Lett.* **1988,** *9*, 1233–1244. **DOI:**10.1080/09593338809384686
41. Y. Gutha, V. S. Munagapati, M. Naushad, K. Abburi, *Desalin.*

Water Treat. 2014, 1–9.
42. Z. D. Reed, M. A. Duncan, *J. Am. Soc. Mass. Spectr.* **2010**, *21*, 739–749. **DOI:**10.1016/j.jasms.2010.01.022
43. G. A. Somorjai, Introduction to Surface Chemistry and Catalysis, Department of Chemistry University of California Berkeley. New York, **1994**.
44. K. P. Huber, G. Herzberg, Molecular Spectra and Molecular Structure IV. Constants of Diatomic Molecules, National Research Council of Canada. Canada, **1978**. **DOI:**10.1007/978-1-4757-0961-2_2
45. J. C. P. Vaghetti, E. C. Lima, B. Royer, B. M. da Cunha, N. F. Cardoso, J. L. Brasil, S. L. P. Dias, *J. Hazard. Mater.* **2009**, *162*, 270–280. **DOI:**10.1016/j.jhazmat.2008.05.039
46. K. Vijayaraghavan, H. Y. N. Winnie, R. Balasubramanian, *Desalinat.* **2011**, *266*, 195–200. **DOI:**10.1016/j.desal.2010.08.026
47. N. Rajic, D. Stojakovic, S. Jevtic, N. Zabukovec, J. Kovac, V. Kaucic, *J. Hazard. Mater.* **2009**, *172*, 1450–1457. **DOI:**10.1016/j.jhazmat.2009.08.011
48. F. Güzel, H. Yakut, G. Topal, *J. Hazard. Mater.* **2008**, *153*, 1275–1287. **DOI:**10.1016/j.jhazmat.2007.09.087
49. A. Uçer, A. Uyanik, S. F. Aygun, *Sep. Purif. Technol.* **2006**, *47*, 113–118. **DOI:**10.1016/j.seppur.2005.06.012
50. Ö. Yavuz, Y. Altunkaynak, F. Güzel, *Water Res.* **2003**, *37*, 948–952. **DOI:**10.1016/S0043-1354(02)00409-8

Povzetek

The adsorption of manganese ions from aqueous solutions by pure and acid-treated *Opuntia ficus indica* as natural low-cost and eco-friendly adsorbents was investigated. The adsorbents' structures were characterized by powder X-ray diffraction and infrared spectroscopy. Specific surface areas were determined using the Brunauer-Emmett-Tell equation. The study was carried out under various parameters influencing the manganese removal efficiency such as pH, temperature, contact time, adsorbent dose and initial concentration of manganese ion. The maximum adsorption capacity reached 42.02 mg/g for acid-treated *Opuntia ficus indica*, and only 20.8 mg/g for pure *Opuntia ficus indica*. The Langmuir, Freundlich and Temkin isotherms equations were tested, and the best fit was obtained by the Langmuir model for both adsorbents. The thermodynamic study shows that chemisorption is the main adsorption mechanism for the activated adsorbent while physisorption is the main adsorption mechanism for the pure adsorbent. The kinetics of the adsorption have been studied using four kinetics models of pseudo-first order, pseudo-second order, Elovich and intra-particle diffusion. Structural analyses indicate the appearance of MnO_x oxides on the cellulose fibers. The adsorption mechanisms consist of an electrostatic interaction followed by oxidation of the Mn (II) to higher degrees, then probably by binding to the surface of the adsorbent by different C-O-MnO_x bonds.